Analysis of the nuclear potential for heavy-ion systems through large-angle quasi-elastic scattering

M. L. Inche Ibrahim,[1,2,*] Muhammad Zamrun,[3] and Hasan Abu Kassim[1,2]
[1]*Quantum Science Center, Faculty of Science, University of Malaya, 50603 Kuala Lumpur, Malaysia*
[2]*Department of Physics, University of Malaya, 50603 Kuala Lumpur, Malaysia*
[3]*Department of Physics, Haluoleo University, Kendari, Sulawesi Tenggara 93232, Indonesia*
(Received 25 April 2012; revised manuscript received 11 January 2013; published 27 February 2013)

A study on the surface diffuseness parameter of the nuclear potential for the reactions of ^{208}Pb with ^{48}Ti, ^{54}Cr, ^{56}Fe, ^{64}Ni, and ^{70}Zn is performed using large-angle quasi-elastic scattering experimental data. Diffuseness parameters that are considerably lower than the standard value of around 0.63 fm are required in order to fit the experimental data at deep sub-barrier energies, except for the ^{54}Cr + ^{208}Pb system, where the required diffuseness parameter is in satisfactory agreement with (but still lower than) the standard value. Furthermore, when the energies of the experimental data used in the fittings are increased from the deep sub-barrier region to the energies closer to the Coulomb barrier height, the best fitted diffuseness parameters also increase. The increase in the obtained diffuseness parameters as the energies are increased also seems to have a possible tendency to be a function of the charge product of the target and projectile nuclei. We find that the phenomenon of threshold anomaly might explain our findings here. The increase in the diffuseness parameters could also due to dynamical effects, for example, due to neutron movements.

DOI: 10.1103/PhysRevC.87.024611 PACS number(s): 25.70.Bc, 21.30.Fe, 24.10.Eq

I. INTRODUCTION

The understanding of the nuclear potential is important in order to describe nucleus-nucleus collisions. The nuclear potential can be studied through both fusion and quasi-elastic scattering. Quasi-elastic scattering is the sum of elastic scattering, inelastic scattering, and nucleon transfer process. Thus, quasi-elastic scattering and fusion are complementary to each other. Large-angle quasi-elastic scattering has been shown to be a valuable way to study the nuclear potential, particularly since large-angle quasi-elastic scattering cross sections are easier and more efficient to be measured experimentally compared to fusion cross sections.

The nuclear potential of the Woods-Saxon form is widely used, and is given by

$$V_N(r) = \frac{-V_0}{1 + \exp[(r - R_0)/a]}, \quad (1)$$

where V_0 is the potential depth, a is the surface diffuseness parameter, and $R_0 = r_0(A_T^{1/3} + A_P^{1/3})$, where r_0 is the radius parameter, while A_T and A_P are the mass numbers of the target and the projectile, respectively. A surface diffuseness parameter of around 0.63 fm is widely accepted [1]. This is supported by recent studies [2–4], where the analyses on the diffuseness parameter were performed using large-angle quasi-elastic scattering experimental data. However, relatively higher diffuseness parameters were required in order to fit fusion experimental data [5]. The cause of the discrepancy is still unclear. More investigations are certainly required in order to further understand the nuclear potential for heavy-ion systems.

At deep sub-barrier energies, channel couplings, which are the couplings between the relative motion and the internal degrees of freedom such as the rotational and vibrational states of the colliding nuclei, weakly influence a nucleus-nucleus collision. Therefore, channel couplings can be justifiably omitted in analyses at deep sub-barrier energies. According to Ref. [2], this is true only for spherical collision systems. All of our studied systems here are spherical, hence, neglecting channel couplings at deep sub-barrier energies should be acceptable. Neglecting channel coupling would simplify the calculations, and could avoid numerical instabilities which would affect the accuracy of the calculations.

Washiyama *et al*. [4] has pointed out that at deep sub-barrier energies, the deviation of the elastic cross sections from the Rutherford cross sections at backward angles is sensitive to the surface region of the nuclear potential, particularly to the surface diffuseness parameter. Thus, an accurate value of the diffuseness parameter could be determined by using large-angle quasi-elastic scattering experimental data at deep sub-barrier energies. However, this could also represent a drawback since small errors in the experimental data could significantly affect the deduced diffuseness parameter. Nonetheless, it is certainly attractive and advantageous to study the diffuseness parameter through large-angle quasi-elastic scattering at deep sub-barrier energies.

In order to make a comprehensive study on the diffuseness parameter, it could be important to make comparisons, for example, between the diffuseness parameters obtained for different charge products of the target and projectile. In light of this, we will perform analyses on the diffuseness parameter at deep sub-barrier energy region and also at another energy region in order to see the effect of collision energies on the deduced diffuseness parameter.

In this article, we carry out a study on the nuclear potential, particularly on the diffuseness parameter, for some heavy-ion systems, namely, the ^{48}Ti, ^{54}Cr, ^{56}Fe, ^{64}Ni, and ^{70}Zn + ^{208}Pb systems, through large-angle quasi-elastic scattering. The procedures of the analyses are explained in Sec. II. In Secs. III and IV, we present the results and the discussion, respectively. The article is then summarized in Sec. V.

*mlukmanibrahim@gmail.com

II. PROCEDURES

The calculations of the quasi-elastic cross sections are performed using CQEL [6], which is a modified version of the computer code CCFULL [7]. In order to find the best fitted value of the diffuseness parameter in comparison with the experimental data, the chi square method χ^2 is used. The experimental data are taken from Ref. [8].

The inclusion of channel couplings in our calculations creates numerical instabilities in varying degrees, which depend on the calculation inputs. This would affect the accuracy of the analyses. Using the computer code, we check and find that quasi-elastic cross sections at energies below the Coulomb barrier height are less influenced by channel couplings and by different coupling schemes compared to quasi-elastic cross sections at energies above the barrier height. Therefore, in order to maximize the accuracy of our analyses, we choose to study and compare the diffuseness parameters obtained at two different energy regions where both regions are below the barrier height.

First, we perform analyses at the deep sub-barrier energy region. For these analyses, only the experimental data with $d\sigma_{\rm qel}/d\sigma_R \geqslant 0.94$ should be included in the fittings [4], where $d\sigma_{\rm qel}/d\sigma_R$ is the ratio of the quasi-elastic to the Rutherford cross sections. Here, we also apply this procedure. As shown later in Sec. III, relatively low values of the diffuseness parameter are needed in order to analyze the experimental data at deep sub-barrier energies. Low values of the diffuseness parameter would produce significant numerical instabilities in the calculations when channel couplings are taken into account, which is undesirable. More importantly, since channel couplings can be neglected at deep sub-barrier energies, we only perform single-channel calculations in the analyses at deep sub-barrier energies.

Second, we perform analyses at what we refer to as the sub-barrier energy region where all the experimental data up to 3 MeV below the Coulomb barrier height V_B are considered in the fittings. For each system in this study, the limit of 3 MeV below the barrier height V_B corresponds to energies between $0.98V_B$ and $0.99V_B$. Both single-channel and coupled-channels calculations are performed in the analyses at sub-barrier energies. The experimental data with $d\sigma_{\rm qel}/d\sigma_R > 1$ are excluded in all fitting procedures, but included in the figures for completeness.

In our calculations, we use an imaginary potential of the Woods-Saxon form with a potential depth of 30 MeV, a radius parameter of 1.0 fm, and a diffuseness parameter of 0.3 fm to simulate compound nucleus formation. The calculations are insensitive to the imaginary parameters provided that the imaginary potential is confined inside the Coulomb barrier. For the real part of the nuclear potential, the radius parameter r_0 is taken to be 1.22 fm. The value of the potential depth V_0 depends on the diffuseness parameter a, where the Coulomb barrier height V_B for each system must be reproduced. The calculations are carried out at a scattering angle of $\theta_{\rm c.m.} = 170^\circ$. The radii of the target and the projectile are taken as $R_T = r_T A_T^{1/3}$ and $R_P = r_P A_P^{1/3}$, respectively, with r_T and r_P taken to be 1.2 fm in order to be consistent with the deformation parameters taken from Refs. [9] and [10]. In order to ensure that the calculations are properly scaled according to the available experimental data, we analyze and plot the calculated ratio of the quasi-elastic to the Rutherford cross sections as functions of effective energies $E_{\rm eff}$ [11,12].

TABLE I. The properties of the single-phonon state for each nucleus. $I, \pi, \hbar\omega$, and β are the angular momentum, parity, excitation energy, and dynamical deformation parameter of the phonon state, respectively.

Nucleus	I^π	$\hbar\omega$ (MeV)	β
^{208}Pb	3^-	2.614	0.110[a]
^{48}Ti	2^+	0.983	0.269[b]
^{54}Cr	2^+	0.834	0.250[b]
^{56}Fe	2^+	0.846	0.239[b]
^{64}Ni	2^+	1.346	0.179[b]
^{70}Zn	2^+	0.884	0.228[b]

[a]From Ref. [9].
[b]From Ref. [10].

In order to perform coupled-channels calculations, the excited states of the colliding nuclei must be considered. The properties of the single-phonon excitation and the deformation parameter for each nucleus are taken from Refs. [9,10], and shown in Table I. The deformation parameter is given by

$$\beta_I = \frac{4\pi}{3ZR_C^I}\left[\frac{B(EI)\uparrow}{e^2}\right]^{1/2}, \qquad (2)$$

where I is the multipolarity, which is associated with the angular momentum of the excited state, $B(EI)\uparrow$ is the electric transition probability, Z is the atomic number, e is the proton charge, and $R_C = r_C A^{1/3}$, where r_C is the Coulomb radius parameter and is taken to be the same as the r_T and r_P, while A is the mass number.

Table II shows the coupling scheme used in the coupled-channels calculations and the Coulomb barrier height for each system (taken from Ref. [13]). For the ^{54}Cr, ^{56}Fe, and ^{64}Ni + ^{208}Pb systems, we use triple-quadrupole phonon and triple-octupole phonon excitations in the projectiles and the targets, respectively. As found by Ref. [14] for the ^{54}Cr + ^{208}Pb system, we find that the mentioned coupling scheme fits the experimental data better than double-quadrupole phonon excitations in the projectiles and triple-octupole phonon excitations in the targets as found by Ref. [13]. For the ^{48}Ti

TABLE II. The coupling scheme used in the coupled-channels calculations and the Coulomb barrier height V_B for each collision system (taken from Ref. [13]). n_P represents the number of quadrupole phonon excitations used in the projectile, while n_T represents the number of octupole phonon excitations used in the target.

System	$[n_P, n_T]$	V_B (MeV)
^{48}Ti + ^{208}Pb	[1,3]	190.50
^{54}Cr + ^{208}Pb	[3,3]	205.50
^{56}Fe + ^{208}Pb	[3,3]	222.50
^{64}Ni + ^{208}Pb	[3,3]	236.25
^{70}Zn + ^{208}Pb	[2,3]	249.30

and $^{70}Zn + ^{208}Pb$ systems, the coupling schemes are taken to be same as found by Ref. [13].

III. RESULTS

A. $^{48}Ti + ^{208}Pb$ system

The best fitted diffuseness parameter for the $^{48}Ti + ^{208}Pb$ system obtained at deep sub-barrier energies through a single-channel calculation is 0.40 fm. The value is clearly considerably lower than the standard value of around 0.63 fm. The calculated ratio of the quasi-elastic to the Rutherford cross sections using $a = 0.40$ fm is shown by the solid line in Fig. 1. The χ^2 value for the best fitted diffuseness parameter in comparison with the experimental data is 0.20, and the required potential depth to reproduce the barrier height is 303.5 MeV.

At sub-barrier energies, the best fitted diffuseness parameter obtained using a single-channel calculation is 0.66 fm, with $\chi^2 = 3.21$ and $V_0 = 82.6$ MeV. This value is consistent with the standard value. The solid line in Fig. 2(a) shows the calculated ratio of the quasi-elastic to the Rutherford cross sections for $a = 0.66$ fm using a single-channel calculation. At energies above the deep sub-barrier region, channel couplings start to play an important role, and should be included in the analysis at sub-barrier energies. Using the coupling scheme as shown in Table II, the best fitted diffuseness parameter obtained at sub-barrier energies through a coupled-channels calculation is 0.43 fm [shown by the solid line in Fig. 2(b)], with $\chi^2 = 1.52$ and $V_0 = 233.5$ MeV. The diffuseness parameter is considerably lower than the standard value. However, from the resulting χ^2 values, the best fitted diffuseness parameter at sub-barrier energies obtained using a coupled-channels calculation fits the experimental data better than the one obtained using a single-channel calculation. Therefore, for the analysis at sub-barrier energies, the best fitted diffuseness parameter obtained through a coupled-channels calculation should be accepted over the one obtained through a single-channel calculation, which is expected.

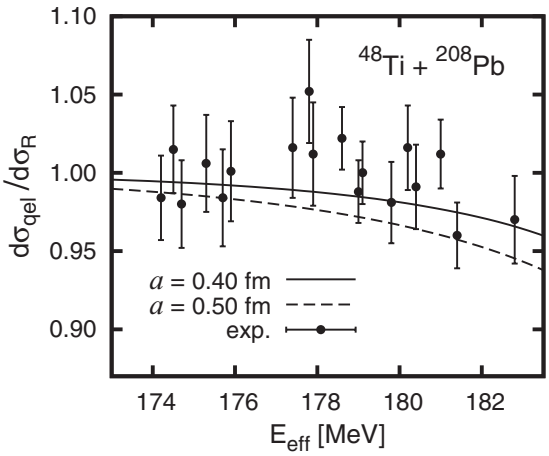

FIG. 1. The ratio of the quasi-elastic to the Rutherford cross sections for the $^{48}Ti + ^{208}Pb$ system at deep sub-barrier energies. The experimental data (taken from Ref. [8]) with $d\sigma_{qel}/d\sigma_R \geqslant 0.94$ are shown and denoted by dots with error bars. The best fitted diffuseness parameter is 0.40 fm, shown by the solid line. The calculation using $a = 0.50$ fm is shown for comparison.

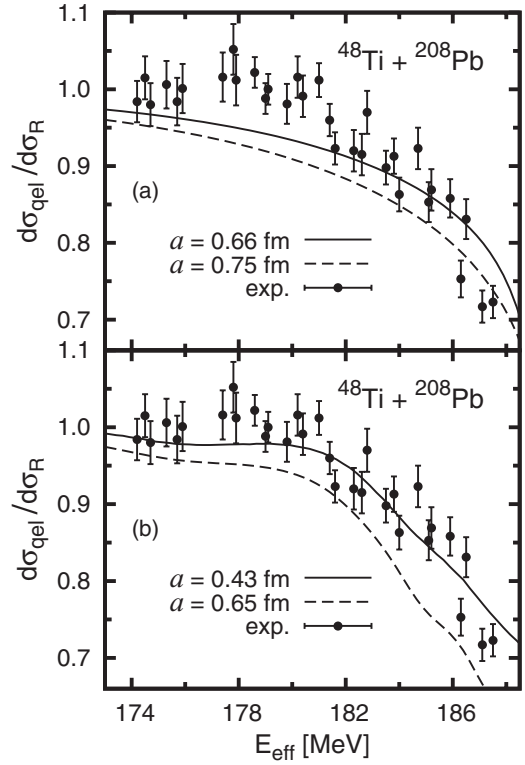

FIG. 2. The ratio of the quasi-elastic to the Rutherford cross sections for the $^{48}Ti + ^{208}Pb$ system at sub-barrier energies. The analyses in (a) the upper and (b) the lower panels are performed using single-channel and coupled-channels calculations, respectively. The experimental data (taken from Ref. [8]) with energies up to 3 MeV below the Coulomb barrier height are shown and denoted by dots with error bars. The best fitted diffuseness parameters obtained using single-channel and coupled-channels calculations are 0.66 and 0.43 fm, respectively. The single-channel and coupled-channels calculations using $a = 0.75$ and 0.65 fm, respectively, are shown for comparison.

B. $^{54}Cr + ^{208}Pb$ system

The best fitted diffuseness parameter for the $^{54}Cr + ^{208}Pb$ system obtained at deep sub-barrier energies through a single-channel calculation is 0.56 fm, which is in good agreement with the standard value. The χ^2 value for the best fitted diffuseness parameter in comparison with the experimental data is 0.18, and the required potential depth to reproduce the barrier height is 114.5 MeV. The calculated ratio of the quasi-elastic to the Rutherford cross sections using $a = 0.56$ fm is shown by the solid line in Fig. 3.

At sub-barrier energies, the best fitted diffuseness parameter obtained using a single-channel calculation is 0.80 fm, with $\chi^2 = 2.05$ and $V_0 = 69.84$ MeV. The best fitted diffuseness parameter is considerably higher than the standard value. The solid line in Fig. 4(a) shows the calculated ratio of the quasi-elastic to the Rutherford cross sections for $a = 0.80$ fm using a single-channel calculation. When a coupled-channels

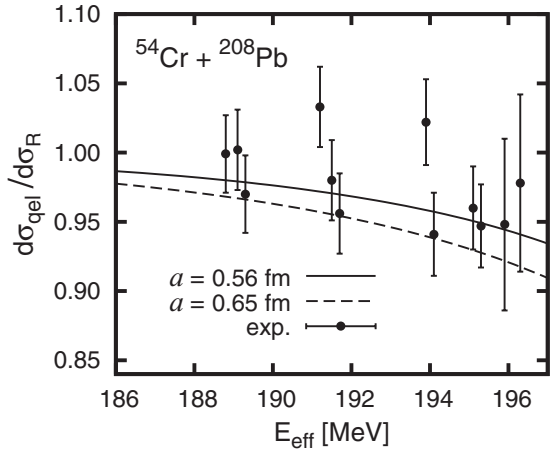

FIG. 3. Same as Fig. 1, but for the ^{54}Cr + ^{208}Pb system. The best fitted diffuseness parameter is 0.56 fm, shown by the solid line. The calculation using $a = 0.65$ fm is shown for comparison.

calculation is used, the best fitted diffuseness parameter obtained at sub-barrier energies is 0.63 fm [shown by the solid line in Fig. 4(b)], with $\chi^2 = 1.36$ and $V_0 = 91.7$ MeV. The obtained diffuseness parameter is in agreement with the standard value. As before, the χ^2 values show that the best fitted diffuseness parameter obtained through a coupled-channels calculation fits the experimental data better than the best fitted diffuseness parameter obtained using a single-channel calculation.

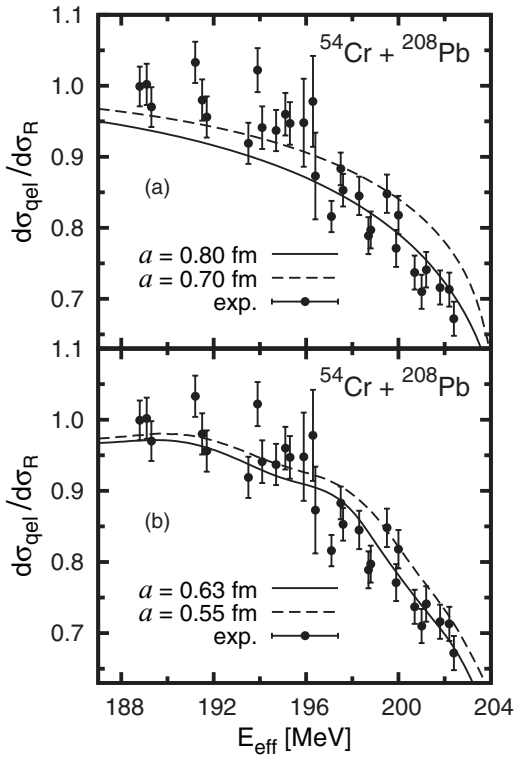

FIG. 4. Same as Fig. 2, but for the ^{54}Cr + ^{208}Pb system. The best fitted diffuseness parameters obtained using single-channel and coupled-channels calculations are 0.80 and 0.63 fm, respectively. The single-channel and coupled-channels calculations using $a = 0.70$ and 0.55 fm, respectively, are shown for comparison.

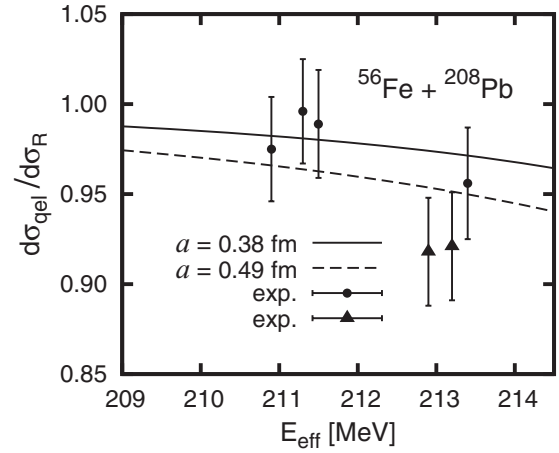

FIG. 5. The ratio of the quasi-elastic to the Rutherford cross sections for the ^{56}Fe + ^{208}Pb system at deep sub-barrier energies. The experimental data (taken from Ref. [8]) with $d\sigma_{qel}/d\sigma_R \geqslant 0.94$ and $0.94 > d\sigma_{qel}/d\sigma_R \geqslant 0.90$ are denoted by dots and triangles with error bars, respectively. The best fitted diffuseness parameters obtained through single-channel calculations using the data with $d\sigma_{qel}/d\sigma_R \geqslant 0.94$ and $d\sigma_{qel}/d\sigma_R \geqslant 0.90$ are 0.38 and 0.49 fm, respectively, shown by the solid line and the dashed line, respectively.

C. ^{56}Fe + ^{208}Pb system

For the ^{56}Fe + ^{208}Pb system, the best fitted diffuseness parameter at deep sub-barrier energies using a single-channel calculation is 0.38 fm, which is significantly lower than the standard value. The χ^2 value for the best fitted diffuseness parameter in comparison with the experimental data is 0.17. The value of the potential depth required to reproduce the barrier height is 355.5 MeV. The calculated ratio of the quasi-elastic to the Rutherford cross sections for $a = 0.38$ fm using a single-channel calculation is shown by the solid line in Fig. 5.

It can be seen in Fig. 5 that there are only four data points available when the analysis is performed using the experimental data with $d\sigma_{qel}/d\sigma_R \geqslant 0.94$. If we include all the experimental data with $d\sigma_{qel}/d\sigma_R \geqslant 0.90$ in the fitting, the best fitted diffuseness parameter obtained using a single-channel calculation is 0.49 fm, with $\chi^2 = 0.76$ and $V_0 = 156$ MeV. This is shown by the dashed line in Fig. 5. The obtained diffuseness parameter is still quite low compared to the standard value of around 0.63 fm.

At sub-barrier energies, the best fitted diffuseness parameter using a single-channel calculation is 0.76 fm, with $\chi^2 = 3.85$ and $V_0 = 74.9$ MeV. The obtained diffuseness parameter is rather high compared to the standard value. The solid line in Fig. 6(a) shows the calculated ratio of the quasi-elastic to the Rutherford cross sections for $a = 0.76$ fm using a single-channel calculation. Using a coupled-channels calculation, the best fitted diffuseness parameter obtained at sub-barrier energies is 0.59 fm, with $\chi^2 = 1.66$ and $V_0 = 103.6$ MeV. The value of the diffuseness parameter is in agreement with the standard value. The solid line in Fig. 6(b) shows the calculated ratio of the quasi-elastic to the Rutherford cross sections for $a = 0.59$ fm using a coupled-channels calculation. Again,

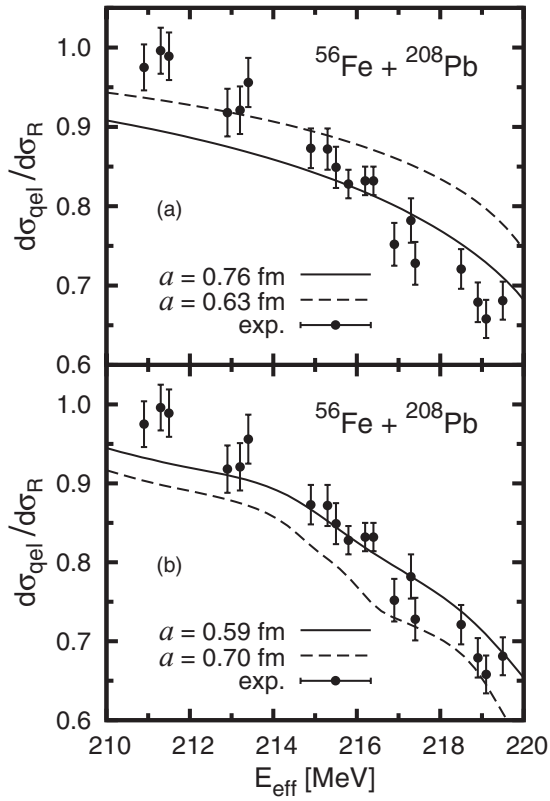

FIG. 6. Same as Fig. 2, but for the ^{56}Fe + ^{208}Pb system. The best fitted diffuseness parameters obtained using single-channel and coupled-channels calculations are 0.76 and 0.59 fm, respectively. The single-channel and coupled-channels calculations using $a = 0.63$ and 0.70 fm, respectively, are shown for comparison.

from the obtained χ^2 values, a coupled-channels calculation is more accurate than a single-channel calculation for the analysis at sub-barrier energies.

D. ^{64}Ni + ^{208}Pb system

The best fitted diffuseness parameter for the ^{64}Ni + ^{208}Pb system obtained at deep sub-barrier energies through a single-channel calculation is 0.32 fm, with $\chi^2 = 0.06$ and $V_0 =$ 752 MeV. The plot for the best fitted diffuseness parameter is indicated by the solid line in Fig. 7. The obtained value is significantly lower than the standard value. In order to reproduce the barrier height, the potential depth also needs to be relatively high.

At sub-barrier energies, the best fitted diffuseness parameter for the ^{64}Ni + ^{208}Pb system obtained using a single-channel calculation is 0.82 fm [shown by the solid line in Fig. 8(a)], with $\chi^2 = 13.28$ and $V_0 = 73.97$ MeV. The obtained diffuseness parameter is clearly considerably higher than the standard value. When a coupled-channels procedure is employed, the best fitted diffuseness parameter is 0.66 fm, which is in agreement with the standard value, with $\chi^2 = 3.99$ and $V_0 = 89.05$ MeV. The solid line in Fig. 8(b) shows the calculated ratio of the quasi-elastic to the Rutherford cross

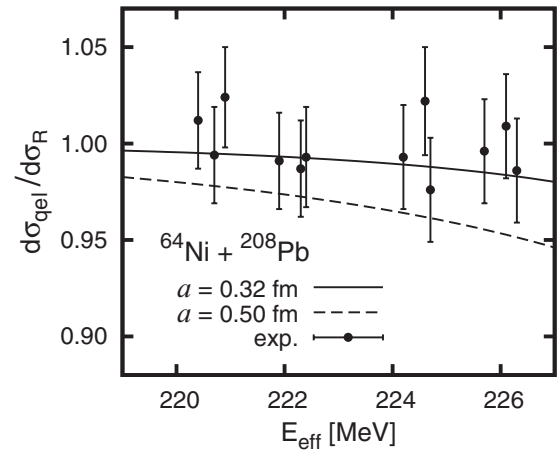

FIG. 7. Same as Fig. 1, but for the ^{64}Ni + ^{208}Pb system. The best fitted diffuseness parameter obtained using a single-channel calculation is 0.32 fm, denoted by the solid line. The single-channel calculation using $a = 0.50$ fm is shown for comparison.

sections for $a = 0.66$ fm using a coupled-channels procedure. It can be seen by comparing Fig. 8(a) with Fig. 8(b) that the best fitted diffuseness parameter obtained through a coupled-

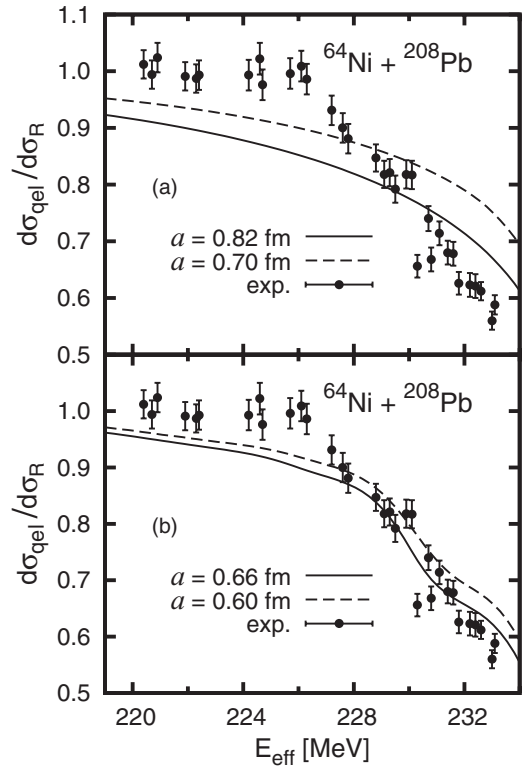

FIG. 8. Same as Fig. 2, but for the ^{64}Ni + ^{208}Pb system. The best fitted diffuseness parameters obtained using single-channel and coupled-channels calculations are 0.82 and 0.66 fm, respectively. The single-channel and coupled-channels calculations using $a = 0.70$ and 0.60 fm, respectively, are shown for comparison.

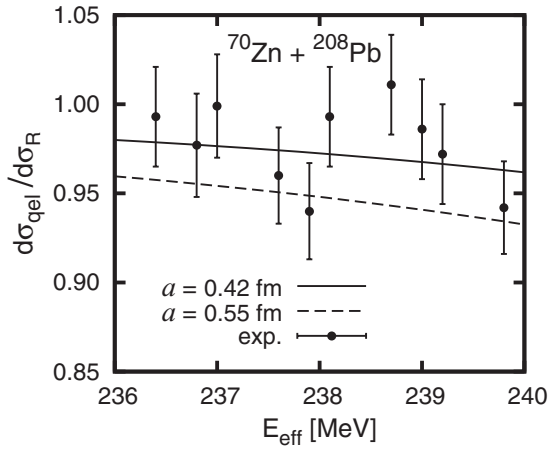

FIG. 9. Same as Fig. 1, but for the ^{70}Zn + ^{208}Pb system. The best fitted diffuseness parameter obtained using a single-channel analysis is 0.42 fm, denoted by the solid line. The single-channel calculation using $a = 0.55$ fm is shown for comparison.

channels procedure fits the experimental better than the best fitted diffuseness parameter obtained through a single-channel procedure. This fact is very clearly indicated by the values of the χ^2 obtained from the analyses.

E. ^{70}Zn + ^{208}Pb

At deep sub-barrier energies, the best fitted diffuseness parameter for the ^{70}Zn + ^{208}Pb system obtained through a single-channel calculation is 0.42 fm, with $\chi^2 = 0.48$ and $V_0 = 302.5$ MeV. The obtained diffuseness parameter is significantly lower than the standard value. The calculated ratio of the quasi-elastic to the Rutherford cross sections for the best fitted diffuseness parameter is shown by the solid line in Fig. 9.

At sub-barrier energies, the best fitted diffuseness parameter for the ^{70}Zn + ^{208}Pb system obtained using a single-channel procedure is 0.64 fm [shown by the solid line in Fig. 10(a)], with $\chi^2 = 2.41$ and $V_0 = 105.5$ MeV. The obtained diffuseness parameter is in agreement with the standard value. However, the results for previous systems show that channel couplings should be considered in the analysis at sub-barrier energies. Using a coupled-channels calculation, the best fitted diffuseness parameter for the ^{70}Zn + ^{208}Pb system at sub-barrier energies is 0.51 fm [shown by the solid line in Fig. 10(b)], with $\chi^2 = 1.11$ and $V_0 = 168.3$ MeV. The best fitted diffuseness parameter is considerably lower than the standard value. However, the best fitted diffuseness parameter at sub-barrier energies obtained through a coupled-channels analysis again fits the experimental data better than the one obtained through a single-channel analysis.

IV. DISCUSSION

For all of the studied systems, the best fitted diffuseness parameters at sub-barrier energies obtained through coupled-channels and single-channel calculations differ considerably. In light of this, the best fitted diffuseness parameters obtained

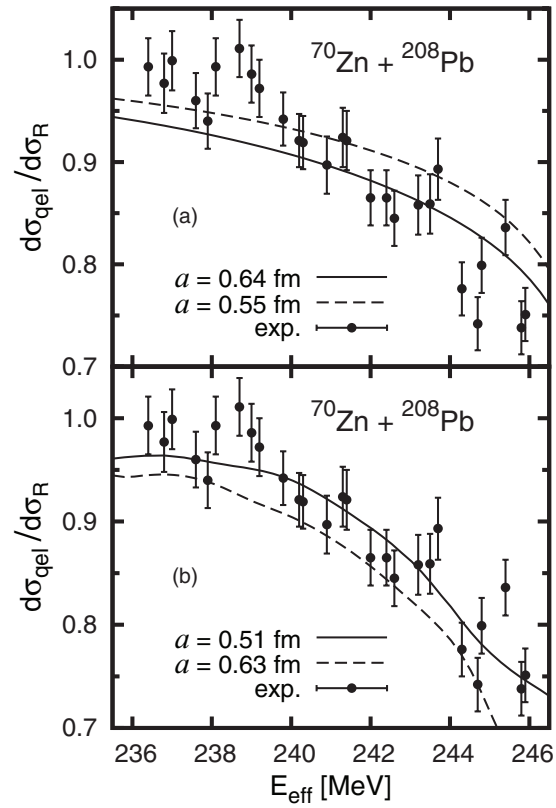

FIG. 10. Same as Fig. 2, but for the ^{70}Zn + ^{208}Pb system. The best fitted diffuseness parameters obtained using single-channel and coupled-channels calculations are 0.64 and 0.51 fm, respectively. The single-channel and coupled-channels calculations using $a = 0.55$ and 0.63 fm, respectively, are shown for comparison.

through coupled-channels calculations are taken as the correct parameters for the analyses at sub-barrier energies since they produce better fits to the experimental data than the ones obtained through single-channel calculations. This is actually expected since the effect of channel couplings is significant and should be taken into account at energies above the deep sub-barrier region. For the ^{56}Fe + ^{208}Pb system, the best fitted diffuseness parameter obtained using the experimental data with $d\sigma_{\rm qel}/d\sigma_R \geqslant 0.94$ is accepted for the analysis at deep sub-barrier energies, even though there are only four data points available. This is mainly because channel couplings might be required in order to analyze the experimental data with $0.90 \leqslant d\sigma_{\rm qel}/d\sigma_R < 0.94$. Figure 11 summarizes the best fitted diffuseness parameter as a function of the charge product of the target and projectile.

At deep sub-barrier energies, the best fitted diffuseness parameters for all of the studied systems are considerably lower than the standard value, except for the ^{54}Cr + ^{208}Pb system, where the best fitted diffuseness parameter can be considered to be in satisfactory agreement with (but still lower than) the standard value. At sub-barrier energies, the best fitted diffuseness parameters for the ^{54}Cr, ^{56}Fe, and ^{64}Ni + ^{208}Pb systems are in good agreement with the standard value. However, the best fitted diffuseness parameters at sub-barrier energies for the ^{48}Ti and ^{70}Zn + ^{208}Pb systems are significantly low and rather low, respectively, compared to the standard

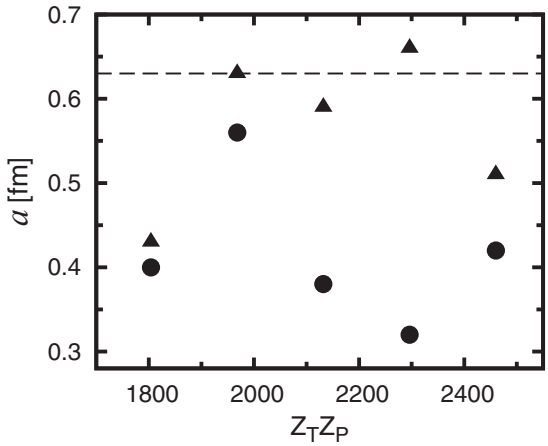

FIG. 11. The best fitted diffuseness parameters at deep sub-barrier energies (denoted by circles) and at sub-barrier energies (denoted by triangles) as functions of charge products of the target and projectile $Z_T Z_P$. The dashed line indicates $a = 0.63$ fm.

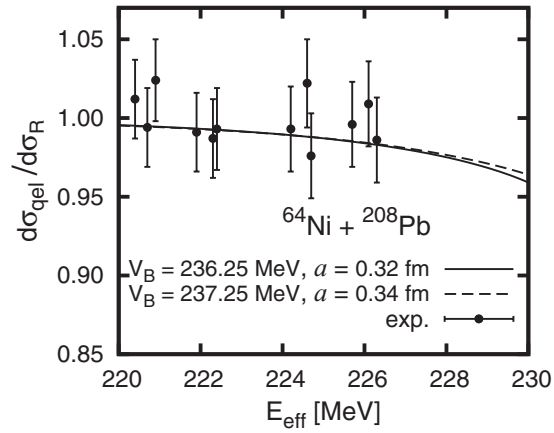

FIG. 12. The calculated ratio of the quasi-elastic to the Rutherford cross sections for the best fitted diffuseness parameters at deep sub-barrier energies for the ^{64}Ni + ^{208}Pb system using two different values of the Coulomb barrier height V_B. When $V_B = 236.25$ and 237.25 MeV are used, the best fitted diffuseness parameters are 0.32 and 0.34 fm, respectively. The calculations are performed using single-channel procedure.

value. It can be seen from Fig. 11 that the best fitted diffuseness parameters obtained at sub-barrier energies are generally quite significantly closer to the standard value compared to the diffuseness parameters obtained at deep sub-barrier energies.

It is also interesting to observe that higher diffuseness parameters are required in order to fit the experimental data as the energies are increased closer to the Coulomb barrier heights. This can be clearly seen in Fig. 11 by comparing the diffuseness parameters obtained at deep sub-barrier energies with the ones obtained at sub-barrier energies. It must be remembered that the fittings at sub-barrier energies also include the data at deep sub-barrier energies. If the data at deep sub-barrier energies are excluded from the fittings at sub-barrier energies, one can see more prominent increases in the best fitted diffuseness parameters. An increase in the diffuseness parameter also leads to a lower potential depth in order to reproduce the barrier height. Therefore, an inconsistency between the diffuseness parameters obtained at the two studied energy regions basically would lead to an inconsistency between values of the potential depth obtained at the studied regions.

It can also be seen from Fig. 11 that there is a possible tendency that a higher charge product of the target and projectile leads to a higher increase in the best fitted diffuseness parameter from the one obtained at deep sub-barrier energies to the one obtained at sub-barrier energies. However, the increase for the ^{70}Zn + ^{208}Pb system is lower than the increases for both the ^{56}Fe and ^{64}Ni + ^{208}Pb systems.

A. Effect of Coulomb barrier height

As found in Ref. [4], we find that a small variation in the value of the Coulomb barrier height V_B has a small effect on the best fitted diffuseness parameter obtained at deep sub-barrier energies. To illustrate this, Fig. 12 compares the best fitted diffuseness parameters at deep sub-barrier energies for the ^{64}Ni + ^{208}Pb system using $V_B = 236.25$ MeV as originally used, with $V_B = 237.25$ MeV. For an increase of 1 MeV in the barrier height from the value that is originally used, the best fitted diffuseness parameter increases by 0.02 fm, from $a = 0.32$ fm to $a = 0.34$ fm. Therefore, slight variations or uncertainties in the values of the barrier height can be dismissed as a cause for the low values of the diffuseness parameter obtained at deep sub-barrier energies.

However, at sub-barrier energies, the effect of the variation of the Coulomb barrier height on the best fitted diffuseness parameter is considerably stronger than the effect at deep sub-barrier energies. For a decrease of 1 MeV in the barrier height from the value that is originally used (i.e., 236.25 MeV), the best fitted diffuseness parameter for the ^{64}Ni + ^{208}Pb system obtained at sub-barrier energies decreases by 0.08 fm, from $a = 0.66$ fm to $a = 0.58$ fm (see Fig. 13). When $V_B = 235.25$ MeV is used, only the experimental data with energies equal to or lower than 232.25 MeV are used in the fittings. Therefore, it is important to accurately and precisely know the value of the barrier height in order to obtain the diffuseness parameter at sub-barrier energies. Furthermore, it is possible that the actual barrier heights are slightly lower than ones that are used here. However, the uncertainty in the barrier heights still cannot account for the discrepancy between the diffuseness parameters obtained at the two studied energy regions, such as the discrepancies for the ^{56}Fe and ^{64}Ni + ^{208}Pb systems.

B. Effect of r_T and r_P

The variations in the target radius parameter r_T and the projectile radius parameter r_P basically have no effect on the calculated quasi-elastic cross sections when using single-channel calculations. This is understandable since varying the r_T and r_P, which would change the radii of the colliding nuclei, mainly affects the deformation parameters [see Eq. (2)] which are not used in a single-channel calculation.

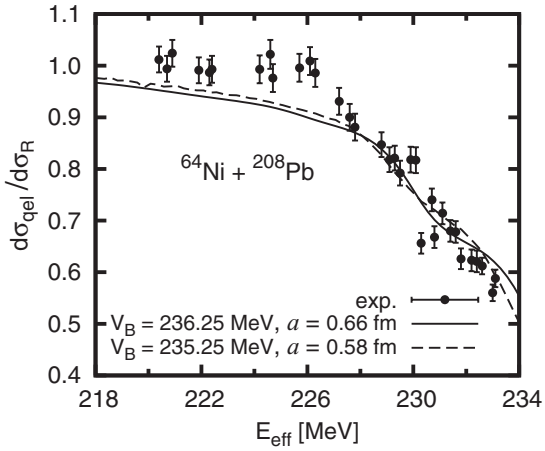

FIG. 13. The calculated ratio of the quasi-elastic to the Rutherford cross sections for the best fitted diffuseness parameters obtained at sub-barrier energies through coupled-channels calculations for the ^{64}Ni + ^{208}Pb system using two different values of the Coulomb barrier height V_B. When $V_B = 236.25$ and 235.25 MeV are used, the best fitted diffuseness parameters are 0.66 and 0.58 fm, respectively.

However, when coupled-channels calculations are used, the effect of varying the r_T and r_P is significant at energies above the deep sub-barrier region. To illustrate this, Fig. 14 shows a comparison between the calculated ratio of the quasi-elastic to the Rutherford cross sections for the ^{64}Ni + ^{208}Pb system using $r_T = r_P = 1.3$ fm and $r_T = r_P = 1.2$ fm. When using $r_T = r_P = 1.3$ fm, the deformation parameters are modified according to Eq. (2) with $\beta_2 = 0.153$ for ^{64}Ni and $\beta_3 = 0.087$ for ^{208}Pb. It can be seen from Fig. 14 that changing r_T and r_P has a very small effect at deep sub-barrier energies, even when coupled-channels calculations are used. Again, this can be explained from the fact that the deformation parameters affect channel couplings, which are weak and can be neglected at deep sub-barrier energies. Hence, the effect of varying r_T and r_P is weak at deep sub-barrier energies. Therefore, the choice

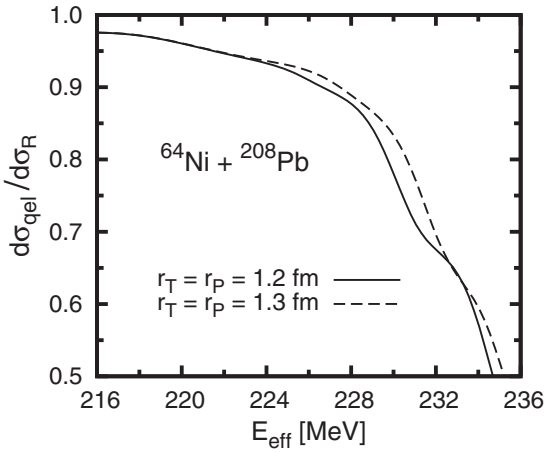

FIG. 14. Comparison between the calculated ratio of the quasi-elastic to the Rutherford cross sections for the ^{64}Ni + ^{208}Pb system using $r_T = r_P = 1.3$ fm (dashed line) and $r_T = r_P = 1.2$ fm (solid line). Both calculations are performed using $a = 0.63$ fm and the coupling scheme as shown in Table II.

in the values of r_T and r_P can be dismissed as a cause for the low values of the diffuseness parameter obtained at deep sub-barrier energies.

Lower r_T and r_P would produce lower calculated quasi-elastic cross sections, particularly at energies above the deep sub-barrier region (see Fig. 14, for example). Hence, a lower diffuseness parameter is required to best fit the experimental data at sub-barrier energies when lower r_T and r_P are used. Therefore, it is possible to make the best fitted diffuseness parameters obtained at sub-barrier energies to be consistent with the ones obtained at deep sub-barrier energies by lowering the values of r_T and r_P appropriately. However, several things must be remembered and considered, and this would present difficulties. First, since all of the studied systems have the same target nucleus, the same r_T should be used. Second, the ranges of r_T and r_P are likely to lie between 1.06 and 1.2 fm [2]. Furthermore, it must be remembered that all of the colliding nuclei here are spherical. Therefore, it is natural to feel that r_P for each projectile nucleus as well as r_T for ^{208}Pb should not differ significantly from each other.

According to the results for the ^{48}Ti + ^{208}Pb system, $r_T \approx 1.2$ fm should be used in order to make the best fitted diffuseness parameters obtained at the two studied energy regions to be consistent with each other. However, when $r_T \approx 1.2$ fm is used for the ^{56}Fe and ^{64}Ni + ^{208}Pb systems, for example, the consistency in the values of the diffuseness parameter at the two studied regions can only be achieved if the r_P's for ^{56}Fe and ^{64}Ni are significantly lower than 1.06 fm. This effort would also make the value of r_T and r_P for each of the studied nucleus to differ significantly. Therefore, an inconsistency in the values of r_T and r_P would be created in order to achieve a consistency in the values of the diffuseness parameter obtained at the two studied energy regions. Furthermore, this effort would also make the best fitted diffuseness parameters obtained at sub-barrier energies to be much more inconsistent with the standard value.

In order to support our discussion above, when $r_T = 1.2$ fm and $r_P = 1.06$ fm are used, the best fitted diffuseness parameter at sub-barrier energies for the ^{56}Fe + ^{208}Pb system using a coupled-channels calculation is 0.57 fm (shown in Fig. 15). As usual, the deformation parameter for ^{56}Fe is modified based on Eq. (2). This means that the value of the best fitted diffuseness parameter is reduced by only 0.02 fm from the value when $r_T = r_P = 1.2$ fm are used. This shows that when $r_T = 1.2$ fm is used, r_P with a value much lower than 1.06 fm is required for the ^{56}Fe + ^{208}Pb system to make the best fitted diffuseness parameter obtained at sub-barrier energies to be consistent with the one obtained at deep sub-barrier energies, if it is possible.

It must be stressed that it is very important to accurately and precisely know r_T and r_P in order to correctly determine the diffuseness parameter at sub-barrier energies. The values of $r_T = r_P = 1.2$ fm that we use here are widely used for the studied nuclei, including by Refs. [9,10]. Therefore, based on the available data that we have, this study suggests that higher values of the diffuseness parameter are required in order to fit the experimental data as the energies increase from the deep sub-barrier region to the energies closer to the Coulomb barrier height.

C. São Paulo potential

From our results, it seems that there is an effect that is not considered in a typical nucleus-nucleus collision (and also in our study here) that makes the nuclear potential appear to be energy dependent. This could be the reason for the diffuseness parameters at deep sub-barrier energies to appear to be considerably lower than the diffuseness parameters at sub-barrier energies and the standard value in general. It was shown that the effect of Pauli nonlocality would make the nuclear potential to be energy dependent [15–17]. For nucleus-nucleus collisions, the nuclear potential due to Pauli nonlocality (called the São Paulo potential $V_{\text{S-P}}$) is given by [15–17]

$$V_{\text{S-P}}(r;E) = V_F(r)\exp\{-\gamma[E - V_C(r) - V_{\text{S-P}}(r;E)]\}, \quad (3)$$

where V_F is the nuclear potential without the effect of Pauli nonlocality, V_C is the Coulomb potential, E is the relative motion energy, and γ is a system-dependent constant.

For heavy-ion systems, the São Paulo potential should be negligible at near-barrier energies since $E \approx V_C(R_B) + V_{\text{S-P}}(R_B)$ [17], where R_B is the location of the barrier height, and γ is very small [16]. From first impressions, it seems that the results found in this study are negligibly affected by the effect of Pauli nonlocality.

However, let us still consider this effect. In order to employ the nuclear potential of Eq. (3), we need the values of γ for our studied systems, which we do not know. For heavy-ion systems, when $V_C + V_{\text{S-P}}$ is small in comparison with E, we can expand Eq. (3) and write [16]

$$V_{\text{S-P}}(r;E) \approx V_F(r)[1 - \gamma E]. \quad (4)$$

From Eq. (4), Ref. [16] showed that

$$V_{\text{S-P}}(r;E) = V_F(r)\left[1 - \lambda\frac{E_{\text{lab}}}{A_P}\right], \quad (5)$$

where λ is a system-independent constant that is equal to 0.0086 MeV^{-1}. Equation (5) enables us to explicitly investigate the effect of Pauli nonlocality in our study. A quick check for the $^{56}\text{Fe} + ^{208}\text{Pb}$ system at $E = 212$ MeV ($E_{\text{lab}} = 269$ MeV) gives $V_{\text{S-P}} = 0.96V_F$. It is important to remember that in this present study, the actual $V_{\text{S-P}}$ should be less energy dependent than Eq. (5) since $V_C + V_{\text{S-P}}$ is not small compared to E. Hence, the actual ratio of $V_{\text{S-P}}/V_F$ for the $^{56}\text{Fe} + ^{208}\text{Pb}$ system at $E = 212$ MeV should be larger than 0.96 (i.e., closer to 1).

In order to explicitly see whether the nuclear potential based on Pauli nonlocality can or cannot explain our results, we replace the Woods-Saxon potential [Eq. (1)] with the São Paulo potential [Eq. (5)] in our calculations. V_F should basically be the double folding potential. However, in order to serve our purpose, which is to study the nuclear potential in the Woods-Saxon form, we use the Woods-Saxon form for V_F in our calculations. Therefore, the São Paulo potential used in our calculations reads

$$V_{\text{S-P}}(r;E) = \frac{-V_0(1 - \lambda E_{\text{lab}}/A_P)}{1 + \exp[(r - R_0)/a]}. \quad (6)$$

As usual, the barrier height must be reproduced in the calculations. Hence, for the same diffuseness parameter, V_0 when using the São Paulo potential [Eq. (6)] is higher than V_0 when using purely the Woods-Saxon potential [Eq. (1)]. For example, for $a = 0.59$ fm, the São Paulo potential requires $V_0 = 108.3$ MeV while the Woods-Saxon potential requires $V_0 = 103.6$ MeV.

Figures 16 and 17 show the results of our calculations for the $^{56}\text{Fe} + ^{208}\text{Pb}$ system. The differences between the quasi-elastic cross sections obtained using the São Paulo potential and the Woods-Saxon potential for the same diffuseness parameter are very small (less than 1%). If all the plots in Figs. 16 and 17 are shown by lines, it is hard to distinguish between the plots using the São Paulo potential and the Woods-Saxon potential for the same diffuseness parameter.

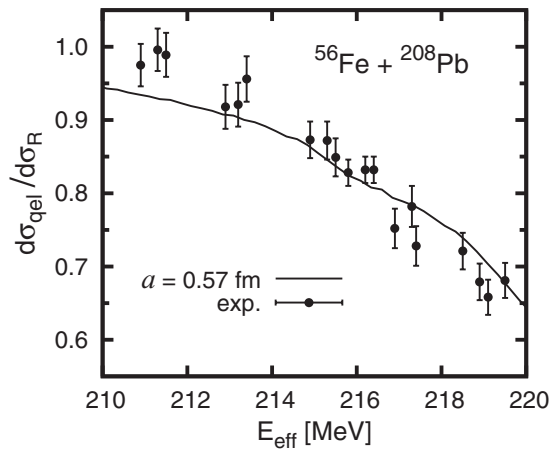

FIG. 15. The calculated ratio of the quasi-elastic to the Rutherford cross sections for the best fitted diffuseness parameter ($a = 0.57$ fm) for the $^{56}\text{Fe} + ^{208}\text{Pb}$ system when $r_T = 1.2$ fm and $r_P = 1.06$ fm are used. The calculation is performed using the coupled-channels procedure as shown in Table II.

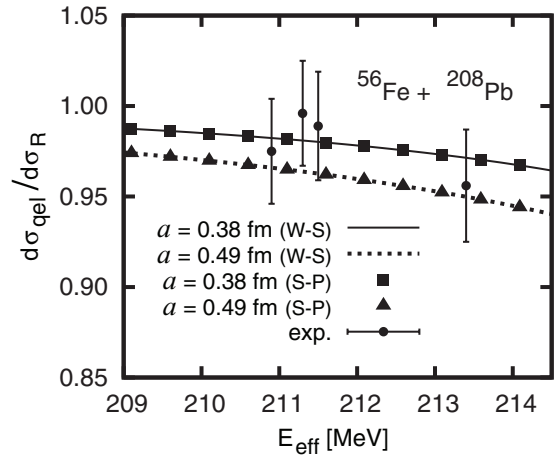

FIG. 16. Same as Fig. 5. W-S and S-P denote the Woods Saxon potential [Eq. (1)] and the São Paulo potential [Eq. (6)], respectively. The plots using the Woods-Saxon potential (solid and dotted lines) are the same as in Fig. 5. The plots using the São Paulo potential shown by squares and triangles are obtained using single-channel calculations with $a = 0.38$ and 0.49 fm, respectively.

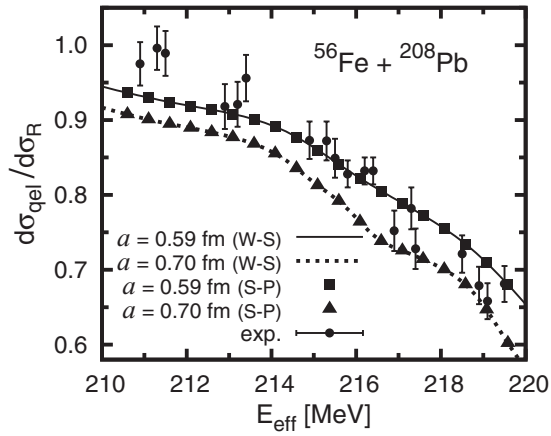

FIG. 17. Same as Fig. 6(b). W-S and S-P denote the Woods Saxon potential [Eq. (1)] and the São Paulo potential [Eq. (6)], respectively. The plots using the Woods-Saxon potential (solid and dotted lines) are the same as in Fig. 6(b). The plots using the São Paulo potential shown by squares and triangles are obtained using coupled-channels calculations (as shown in Table II) with $a = 0.59$ and 0.70 fm, respectively.

If the effect of Pauli nonlocality is able to explain the relatively low diffuseness parameter obtained at deep sub-barrier energies, then the best fitted diffuseness parameter should be consistent with the standard value when using the $V_{\text{S-P}}$ [Eq. (6)]. However, we show that the $V_{\text{S-P}}$ still produces a best fitted diffuseness parameter that is considerably lower than the standard value (practically the same as the best fitted diffuseness parameter when using purely the Woods-Saxon potential). Similarly, if the Pauli nonlocality is able to explain the discrepancy found in this study, then $V_{\text{S-P}}$ [Eq. (6)] should produce (almost) the same best fitted diffuseness parameter when fitting the experimental data at deep sub-barrier energies and when fitting the data at sub-barrier energies. However, the calculations show that this is not the case. In conclusion, we demonstrate that the effect of Pauli nonlocality is clearly negligible in our study.

D. Effect of threshold anomaly

One of the well-known phenomena in the scattering of heavy ions is the threshold anomaly [18]. This phenomenon is related to the variation of the real part of the nuclear potential due to a dispersion relation that arises from the causality principle [19]. The dispersion relation takes the form [18,19]

$$\Delta V_N(r;E) = \frac{\mathrm{P}}{\pi}\int_0^\infty \frac{W_N(r;E')}{E'-E}dE', \tag{7}$$

where P denotes principal value, W_N is the imaginary part of the nuclear potential, and ΔV_N is the real part of the nuclear potential that depends on the imaginary part.

If the effect of the threshold anomaly is present and influences the studied collisions, then the nuclear potential obtained from the fitting of the experimental data at deep sub-barrier energies $V_{N(\text{deep})}$ can be written as

$$V_{N(\text{deep})}(r;E) = V_{N(\text{O})}(r) + \Delta V_{N(\text{deep})}(r;E), \tag{8}$$

where $\Delta V_{N(\text{deep})}$ is ΔV_N at the deep sub-barrier region, and $V_{N(\text{O})}$ is the original nuclear potential that is not affected by the threshold anomaly. For the nuclear potential obtained through the fitting of experimental data, E in Eqs. (7) and (8) can be regarded as the average energy of the experimental data points that are used in the fitting.

Unfortunately, we do not have the experimental data to determine W_N as a function of energy. Thus, the actual value of $\Delta V_{N(\text{deep})}$ cannot be determined. However, if $|W_N|$ (where $W_N \leqslant 0$) rises rapidly as a function of energy over some energy range, the contribution to ΔV_N will be attractive ($\Delta V_N < 0$) in that same energy range [19].

For all nucleus-nucleus collisions, it is natural to think that $|W_N|$ (where $W_N \leqslant 0$) definitely rises from (almost) zero at energies well below the barrier height to some value at energies in the vicinity of the barrier height, and this value of $|W_N|$ is approximately maintained for all energies above the barrier height. This behavior of W_N has been shown by many studies [18–21]. Therefore, generally speaking, the integral of Eq. (7) leads to a negative (attractive) ΔV_N (since $W_N \leqslant 0$). Furthermore, the dispersion relation makes the modulus of the real part of the nuclear potential to have a bell-shaped maximum in the vicinity of the Coulomb barrier height [18,19]. Hence, the contribution by the dispersion relation at $E = V_B$ should be stronger (more negative) than the contribution at deep sub-barrier energies. From Eq. (8), we can generally write

$$V_{N(\text{deep})} - V_{N(\text{O})} \leqslant 0, \tag{9}$$

where less than zero and equals to zero indicate the presence and the absence of the threshold anomaly at deep sub-barrier energies, respectively.

Now, let us use the results for the ^{56}Fe + ^{208}Pb system to illustrate our discussion. Using the best fitted diffuseness parameter and the required potential depth to reproduce the barrier height (as obtained in Sec. III), we can write the best fitted nuclear potential at deep sub-barrier energies as

$$V_{N(\text{deep})}(r) = -\frac{355.5}{1+\exp[(r-11.9\ \text{fm})/0.38\ \text{fm}]}\ \text{MeV}. \tag{10}$$

In order to explain the relatively low diffuseness parameter obtained at deep sub-barrier energies, our aim is to see that the $V_{N(\text{O})}$ has a diffuseness parameter that agrees with the standard value. Let us say that the $V_{N(\text{O})}$ has $a = 0.63$ fm, and the required potential depth to reproduce the barrier height for the ^{56}Fe + ^{208}Pb system when $a = 0.63$ fm is 92.85 MeV (without considering the contribution by the dispersion relation). It is important to notice that if there is a contribution by the dispersion relation at barrier height energy ($E = V_B$), the potential depth should be lower than 92.85 MeV in order to reproduce the barrier height. For now, let us write the $V_{N(\text{O})}$ for the ^{56}Fe + ^{208}Pb system as

$$V_{N(\text{O})}(r) = -\frac{V_0}{1+\exp[(r-11.9\ \text{fm})/0.63\ \text{fm}]}\ \text{MeV}. \tag{11}$$

Let us evaluate the nuclear potentials at $r = 14.4$ fm, which is approximately the turning point for the average deep sub-barrier energies of our experimental data. This gives $V_{N(\text{deep})} = -0.49$ MeV and $V_{N(\text{O})} = -1.72$ MeV when the V_0 for Eq. (11)

is 92.85 MeV. It can be seen that when $V_0 = 92.85$ MeV (i.e., without considering the contribution by the dispersion relation), the $V_{N(O)}$ of Eq. (11) does not satisfy Eq. (9).

However, as mentioned before, the V_0 for Eq. (11) could be lower than 92.85 MeV due to the contribution by the dispersion relation. For example, if the threshold anomaly is negligible at deep sub-barrier energies but very strong at $E = V_B$, Eq. (9) can be satisfied at $r = 14.4$ fm if the V_0 for Eq. (11) is approximately 26.5 MeV. Hence, we show that the threshold anomaly could explain the relatively low diffuseness parameters obtained at deep sub-barrier energies, or at least make the $V_{N(O)}$ to have a higher diffuseness parameter than the one obtained at deep sub-barrier energies. This is due to the fact that the contribution by the dispersion relation at $E = V_B$ is stronger than the contribution at deep sub-barrier energies. However, a more detailed analysis must be done in order to know the actual contribution by the dispersion relation for each of the studied systems. This is required in order to see whether the dispersion relation can lead the $V_{N(O)}$ to have a diffuseness parameter that agrees or disagrees with the standard value.

Now let us see if the effect of the threshold anomaly can explain the discrepancy between the diffuseness parameters obtained at sub-barrier and deep sub-barrier energies. Since the sub-barrier region should effectively be closer to the location of the bell-shaped maximum than the deep sub-barrier region, $|\Delta V_{N(\mathrm{sub})}| > |\Delta V_{N(\mathrm{deep})}|$, where $\Delta V_{N(\mathrm{sub})}$ is ΔV_N at sub-barrier region. The nuclear potential obtained from the fitting of the experimental data at sub-barrier energies $V_{N(\mathrm{sub})}$ can be written as

$$V_{N(\mathrm{sub})} = V_{N(O)} + \Delta V_{N(\mathrm{sub})}. \tag{12}$$

In order to eliminate the discrepancy, the $V_{N(O)}$'s in Eqs. (8) and (12) should be the same. Eliminating the $V_{N(O)}$ through Eqs. (8) and (12), and using the fact that $\Delta V_{N(\mathrm{sub})}$ is more negative than $\Delta V_{N(\mathrm{deep})}$, we can write

$$V_{N(\mathrm{sub})} - V_{N(\mathrm{deep})} < 0. \tag{13}$$

From the result in Sec. III, we can write the $V_{N(\mathrm{sub})}$ for the $^{56}\mathrm{Fe} + ^{208}\mathrm{Pb}$ system as

$$V_{N(\mathrm{sub})}(r) = -\frac{103.6}{1 + \exp[(r - R_{\mathrm{sub}})/0.59\ \mathrm{fm}]}\ \mathrm{MeV}. \tag{14}$$

The R_{sub} in Eq. (14) is the sum of R_0 and coupling components due to vibrational excitations, and should therefore be slightly higher than 11.9 fm. However, let us also use $R_{\mathrm{sub}} = 11.9$ fm since this would not invalidate our discussion here. Evaluating $V_{N(\mathrm{sub})}$ [Eq. (14)] and $V_{N(\mathrm{deep})}$ [Eq. (10)] at $r = 15$ fm, we get $V_{N(\mathrm{sub})} - V_{N(\mathrm{deep})} = -0.437$ MeV. Therefore, Eq. (13) is satisfied and it is thus possible to eliminate or at least reduce the discrepancy through the dispersion relation. However, again, it is important to know the actual contribution by the dispersion relation, so we can determine how much the discrepancy can be reduced.

E. Dynamical effects

It is also likely that the discrepancy could due to the same factors that might cause the diffuseness parameters obtained through fusion experimental data to be higher than those obtained through scattering experimental data (see Ref. [5]). In a fusion process, the colliding nuclei would penetrate deeper into the nuclear potential region than in scattering. Similarly, the colliding nuclei generally approach each other closer in scattering at sub-barrier energies than in scattering at deep sub-barrier energies. Hence, it is apparent to make a connection between the obtained diffuseness parameters and how close the colliding nuclei approach each other.

Reference [5] has discussed several reasons that might cause the discrepancy between the diffuseness parameters obtained through fusion and scattering. One reason that might be related to scatterings at different energies is the dynamical effects, particularly regarding neutron movements towards the other nucleus when the colliding nuclei come close together. This would reduce the dynamical barrier compared to the normal static barrier [22]. The reduction in the barrier clearly would increase the fusion cross sections, thus decreasing the scattering cross sections.

So, if the neutron movements are stronger at sub-barrier energies than at deep sub-barrier energies, then the scattering cross sections obtained at sub-barrier energies would be lower than expected in comparison with the scattering cross sections at deep sub-barrier energies. As can be seen from the calculations (see Sec. III), a higher diffuseness parameter is required in order to fit experimental data with lower quasi-elastic cross sections for given energies. This could at least partly explain the increase in the diffuseness parameters obtained in this present study as the energies increase.

V. SUMMARY

The surface diffuseness parameters of the nuclear potential for heavy-ion systems of the ^{48}Ti, ^{54}Cr, ^{56}Fe, ^{64}Ni, and $^{70}\mathrm{Zn} + ^{208}\mathrm{Pb}$ reactions have been studied through large-angle quasi-elastic scattering at sub-barrier and deep sub-barrier energies. At deep sub-barrier energies, the diffuseness parameters required to fit the experimental data are between 0.32 and 0.56 fm. The deduced diffuseness parameters for all of the studied systems are clearly significantly lower than the standard value of around 0.63 fm, except for the $^{56}\mathrm{Cr} + ^{208}\mathrm{Pb}$ system, where the best fitted diffuseness parameter is in satisfactory agreement with (but still lower than) the standard value. We find that the phenomenon of threshold anomaly might explain the relatively low diffuseness parameters obtained at deep sub-barrier energies. However, the actual contribution of the dispersion relation must be known in order to know how well we can explain the results.

At sub-barrier energies, the diffuseness parameters required to fit the experimental data are between 0.43 and 0.66 fm. The diffuseness parameters obtained at sub-barrier energies agree with the standard value better than the ones obtained at deep sub-barrier energies. It is found that the target radius parameter r_T, the projectile radius parameter r_P, and the Coulomb barrier height V_B play quite significant roles in determining the diffuseness parameters at sub-barrier energies.

Our results also show that higher diffuseness parameters are required in order to fit the experimental data as the energies are increased from the deep sub-barrier region to the energies closer to the Coulomb barrier height. The increase in the best fitted diffuseness parameters occurs for all of the studied collision systems. The increase in the diffuseness parameters also leads to the decrease in the potential depths. There is also a possible tendency that a higher charge product of the target and projectile leads to a higher increase in the best fitted diffuseness parameter from the one obtained at deep sub-barrier energies to the one obtained at sub-barrier energies.

We show that the effect of Pauli nonlocality is negligible in this present study. In contrast, we find that the phenomenon of threshold anomaly could at least reduce the discrepancy between the diffuseness parameters obtained at the two studied regions. It is also possible that the discrepancy is due to the same factors that might cause the diffuseness parameters obtained through fusion experimental data to be higher than those obtained through scattering experimental data [5], particularly regarding neutron movements. Experimental data that enable the determination of the actual contribution by the dispersion relation on the studied systems will be helpful for future studies. Further studies on many other collision systems will also be helpful to support or disprove our findings here.

ACKNOWLEDGMENTS

The authors would like to thank the University of Malaya for financial support through PPP (No. PS329/2009C) and UMRG (No. RG119/10AFR) grants. This work is also supported by Fundamental Research Grant 2011 for Higher Education from the Ministry of National Education, the Republic of Indonesia.

[1] R. A. Broglia and A. Winther, *Heavy Ion Reactions (Lecture Notes), Volume 1: Elastic and Inelastic Reactions* (Benjamin/Cummings, San Francisco, 1981), p. 114.
[2] L. R. Gasques, M. Evers, D. J. Hinde, M. Dasgupta, P. R. S. Gomes, R. M. Anjos, M. L. Brown, M. D. Rodriguez, R. G. Thomas, and K. Hagino, Phys. Rev. C **76**, 024612 (2007).
[3] M. Evers, M. Dasgupta, D. J. Hinde, L. R. Gasques, M. L. Brown, R. Rafiei, and R. G. Thomas, Phys. Rev C **78**, 034614 (2008).
[4] K. Washiyama, K. Hagino, and M. Dasgupta, Phys. Rev. C **73**, 034607 (2006).
[5] J. O. Newton, R. D. Butt, M. Dasgupta, D. J. Hinde, I. I. Gontchar, C. R. Morton, and K. Hagino, Phys. Rev. C **70**, 024605 (2004).
[6] K. Hagino *et al*. (unpublished).
[7] K. Hagino, N. Rowley, and A. T. Kruppa, Comput. Phys. Commun. **123**, 143 (1999).
[8] S. Mitsuoka, H. Ikezoe, K. Nishio, K. Tsuruta, S. C. Jeong, and Y. Watanabe, Phys. Rev. Lett. **99**, 182701 (2007).
[9] T. Kibedi and R. H. Spears, At. Data Nucl. Data Tables **80**, 35 (2002).
[10] S. Raman, C. W. Nestor, and P. Tikkanen, At. Data Nucl. Data Tables **78**, 1 (2001).
[11] K. Hagino and N. Rowley, Phys. Rev. C **69**, 054610 (2004).
[12] H. Timmers, J. R. Leigh, M. Dasgupta, D. J. Hinde, R. C. Lemon, J. C. Mein, C. R. Morton, J. O. Newton, and N. Rowley, Nucl. Phys. A **584**, 190 (1995).
[13] Muhammad Zamrun F., K. Hagino, S. Mitsuoka, and H. Ikezoe, Phys. Rev. C **77**, 034604 (2008).
[14] Muhammad Zamrun F. and Hasan Abu Kasim, AIP Conf. Proc. **1328**, 74 (2012).
[15] M. A. Cândido Ribeiro, L. C. Chamon, D. Pereira, M. S. Hussein, and D. Galetti, Phys. Rev. Lett. **78**, 3270 (1997).
[16] L. C. Chamon, D. Pereira, M. S. Hussein, M. A. Cândido Ribeiro, and D. Galetti, Phys. Rev. Lett. **79**, 5218 (1997).
[17] L. C. Chamon, B. V. Carlson, L. R. Gasques, D. Pereira, C. DeConti, M. A. G. Alvarez, M. S. Hussein, M. A. Cândido Ribeiro, E. S. Rossi, and C. P. Silva, Phys. Rev. C **66**, 014610 (2002).
[18] G. R. Satchler, Phys. Rep. **199**, 147 (1991).
[19] C. Mahaux, H. Ngo, and G. R. Satchler, Nucl. Phys. A **449**, 354 (1986).
[20] W. Y. So, T. Udagawa, K. S. Kim, S. W. Hong, and B. T. Kim, Phys. Rev. C **76**, 024613 (2007).
[21] W. Y. So, T. Udagawa, S. W. Hong, and B. T. Kim, Phys. Rev. C **77**, 024609 (2008).
[22] A. Iwamoto and K. Harada, Z. Phys. A **326**, 201 (1987).